

ORIGINAL RESEARCH

 OPEN ACCESS

## Impact of myeloid-derived suppressor cell on Kupffer cells from mouse livers with hepatocellular carcinoma

Stéphanie Lacotte<sup>a</sup>, Florence Slits<sup>a</sup>, Lorenzo A. Orci<sup>a</sup>, Jeremy Meyer<sup>b</sup>, Graziano Oldani<sup>a</sup>, Vaihere Delaune <sup>a</sup>, Carmen Gonelle-Gispert<sup>b</sup>, Philippe Morel<sup>b,c</sup> and Christian Toso<sup>a,c</sup>

<sup>a</sup>Hepatology and Transplantation Laboratory, Division of Abdominal and Transplantation Surgery, Department of Surgery, Geneva University Hospitals and Faculty of Medicine, Geneva, Switzerland; <sup>b</sup>Surgical Research Unit, Division of Abdominal and Transplantation Surgery, Department of Surgery, Geneva University Hospitals and Faculty of Medicine, Geneva, Switzerland; <sup>c</sup>Hepato-pancreato-biliary Centre, Geneva University Hospitals, Geneva, Switzerland

### ABSTRACT

Kupffer cells represent the first line of defense against tumor cells in the liver. Myeloid-derived suppressor cells (MDSC) have recently been observed in the liver parenchyma of tumor-bearing animals. The present study investigates the function of the MDSC subsets, and their impact on Kupffer cell phenotype and function. RIL-175 mouse hepatocellular carcinoma (HCC) cells were injected into the median liver lobe of C57BL/6 mice. Three weeks later, the median lobe hosting the tumor nodule was removed, and Kupffer cells and MDSCs were sorted from the remaining liver. Mouse livers devoid of HCC served as control. Kupffer cells expressed less co-stimulatory CD86 and MHCII and more co-inhibitory CD274 molecules in HCC-bearing livers than in control livers. Corresponding to this phenotype, Kupffer cells from HCC-bearing mice were less efficient in their function as antigen-presenting cells. Three CD11b<sup>+</sup> cell populations were identified and sorted from HCC-bearing mice. These cells had various phenotypes with different levels of MDSC-specific surface markers (Ly6G<sup>high</sup> cells, Gr1<sup>high</sup> cells, and Ly6C<sup>low</sup> cells), and may be considered as bonafide MDSCs given their suppression of antigen-specific T cell proliferation. Primary isolated Kupffer cells in co-culture with the three MDSC subsets showed a decrease in CCL2 and IL-18 secretion, and an increase in IL-10 and IL-1 $\beta$  secretion, and an increased expression of CD86, CD274, and MHCII. In conclusion, these data demonstrated the existence of three MDSC subsets in HCC-bearing animals. These cells altered Kupffer cell function and may decrease the migration and activation of anticancer effector cells in the liver.

**Abbreviations:** CFSE, carboxyfluorescein succinimidyl ester; HCC, hepatocellular carcinoma; LPS, lipopolysaccharide; MDSC, myeloid-derived suppressor cells; MHC, major histocompatibility complex; PD-L1, programmed death-ligand 1

### ARTICLE HISTORY

Received 2 December 2015  
Revised 5 September 2016  
Accepted 5 September 2016

### KEYWORDS



Antigen-presentation; co-stimulation; HCC; MDSC


### Introduction

The liver includes a unique micro-environment with an adaptive immune response favoring the induction of immunological tolerance rather than immunity.<sup>1</sup> In this context, sessile resident liver macrophages, Kupffer cells, represent an important line of defense against nanoparticles, viruses, and tumor cells.<sup>2</sup> Kupffer cells express MHC class I and class II, as well as co-stimulatory molecules, and are able to initiate an antigen-specific immune response.<sup>3,4</sup> A number of authors have studied the role of Kupffer cells in viral infections, after ischemia-reperfusion injury, and in the context of non-alcoholic fatty liver disease. In liver cancer, the role of Kupffer cells remains controversial,<sup>5-7</sup> mainly due to difficulties in distinguishing between different macrophages subsets. Most resident Kupffer cells are derived from yolk sac and/or fetal liver progenitor cells and maintain their pool by self-renewal, independently from bone marrow-derived monocytes and hematopoiesis. Kupffer cells are radio-

resistant, long-lived, and are present in the liver both under steady-state and inflammatory conditions,<sup>8-10</sup> whereas infiltrating bone marrow-derived monocytes undergo recruitment and clearance thanks to signals promoting the activation and the resolution of inflammation, respectively. Furthermore, Kupffer cells demonstrate phagocytic and cytokine-producing capacities, which differ from those shown by infiltrating macrophages.<sup>9</sup>

The ability of Kupffer cells to act as antigen-presenting cells can be modulated by innate signals, including toll-like receptor ligands, cytokines, and reactive oxygen species, but also by the interaction with other cell types.<sup>3,11</sup> Among such interacting cells, myeloid derived-suppressor cells (MDSC) are a heterogeneous population of immature myeloid cells, which infiltrate the liver in the presence of soluble inflammatory factors including GM-CSF, VEGF, IL-6, IL-1 $\beta$ , and CCL2.<sup>12</sup> MDSCs demonstrate an intense immune suppressive activity in both tumor and infection models, as shown by the inhibitory interaction between Gr1<sup>+</sup> CD11b<sup>+</sup>

**CONTACT** Stéphanie Lacotte  [stephanie.lacotte@unige.ch](mailto:stephanie.lacotte@unige.ch)  Division of Abdominal and Transplantation Surgery, Department of Surgery, 4 rue Gabrielle Perret-Gentil, 1211 Geneva.

 Supplemental data for this article can be accessed on the [publisher's website](#).

Published with license by Taylor & Francis Group, LLC © Stéphanie Lacotte, Florence Slits, Lorenzo A. Orci, Jeremy Meyer, Graziano Oldani, Vaihere Delaune, Carmen Gonelle-Gispert, Philippe Morel and Christian Toso.

This is an Open Access article distributed under the terms of the Creative Commons Attribution-Non-Commercial License (<http://creativecommons.org/licenses/by-nc/3.0/>), which permits unrestricted non-commercial use, distribution, and reproduction in any medium, provided the original work is properly cited. The moral rights of the named author(s) have been asserted.

MDSCs, and T and NK cells.<sup>13,14</sup> In addition, MDSCs suppress cytokine (IL-12 and IL-6) production by macrophages.<sup>15,16</sup> These observations have been gathered utilizing peritoneal macrophages rather than resident Kupffer cells, with MDSCs sorted as Gr1<sup>+</sup> CD11b<sup>+</sup> cells. Moreover, the role of MDSC sub-types on Kupffer cells in the presence of hepatocellular carcinoma (HCC) remains poorly defined.<sup>17,18</sup>

Using an *in vivo* mouse model of HCC, we aimed (1) to assess the phenotype and activation level of Kupffer cells in the presence of HCC, (2) to characterize all involved MDSC subsets in such a model, and (3) to explore the effect of MDSCs on Kupffer cell phenotype and function.

## Results

### Kupffer cells in HCC and in the liver parenchyma surrounding the tumor

In order to specifically study Kupffer cells (and not circulating macrophages), we have developed a protocol of *in vivo* liver

perfusion, non-parenchymal cells isolation, and specific flow cytometry-labeling strategy (Fig. 1A). Liver mononuclear cells were isolated from livers of control and HCC-bearing mice, and F4-80<sup>high</sup> MHCII<sup>+</sup> cells were identified. To exclude Kupffer cell/endothelial cell doublets (some are not excluded in the classical SSC-Height/SSC-Area plot), an anti-CD68 membrane labeling was performed. CD68 is highly expressed at the surface of endothelial cells, and primarily in the cytoplasm of Kupffer cells<sup>19</sup> and data not shown). Single Kupffer cells were therefore selected as CD68<sup>low</sup> cells. In addition, the selected population did not express Ly6C, while circulating macrophages do express this marker.<sup>20,21</sup>

We further analyzed whether Kupffer cells in the liver lobes harboring HCC expressed positive and negative co-stimulatory molecules differently than Kupffer cells residing in non-tumorous liver lobes (surrounding parenchyma) or in control livers (Fig. 1B). CD86 expression was lower in both tumor-bearing and surrounding liver parenchyma compared to controls (Mean Fluorescence Intensity [MFI]: 75 and 99.9, respectively, compared to 158 in controls). In contrast, CD274 (also known as

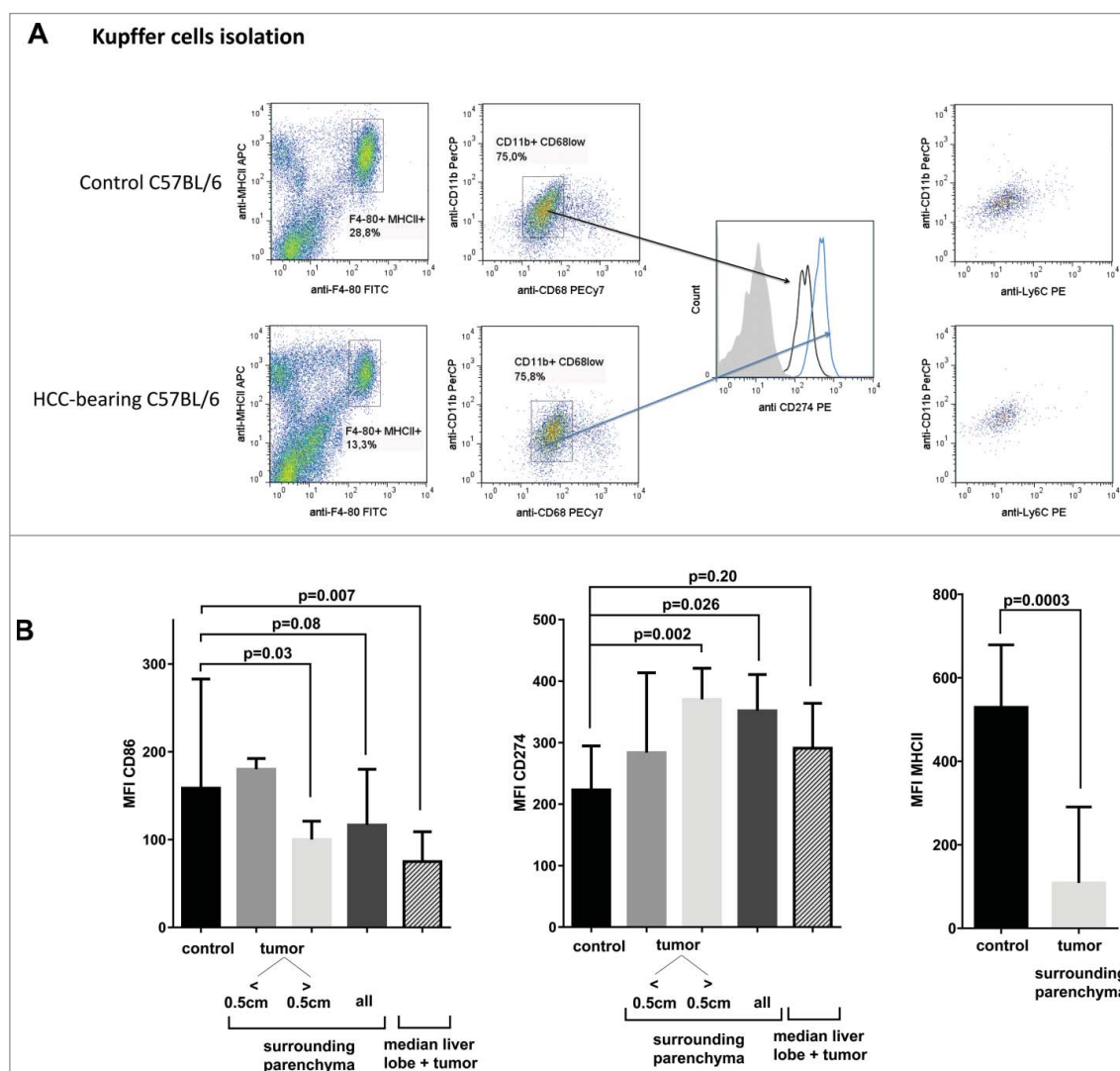


**Figure 1.** Kupffer cells phenotype in the liver of control and HCC-bearing mice. (A) Liver mononuclear cells were isolated by *in vivo* liver digestion and F4-80<sup>high</sup> MHCII<sup>+</sup> cells were assessed. Single Kupffer cells were therefore selected as CD68<sup>low</sup> and Ly6C<sup>-</sup> cells. The expression of the positive and negative co-stimulatory molecules CD86 and CD274 (PD-L1) was assessed. (B) CD86, CD274, and MHCII expression levels in Kupffer cells from control HCC-free mouse liver, and from the surrounding parenchyma from mice with tumor of less or more than 0.5 cm diameter, and from the HCC-bearing median lobe. (MFI: Mean Fluorescence Intensity).

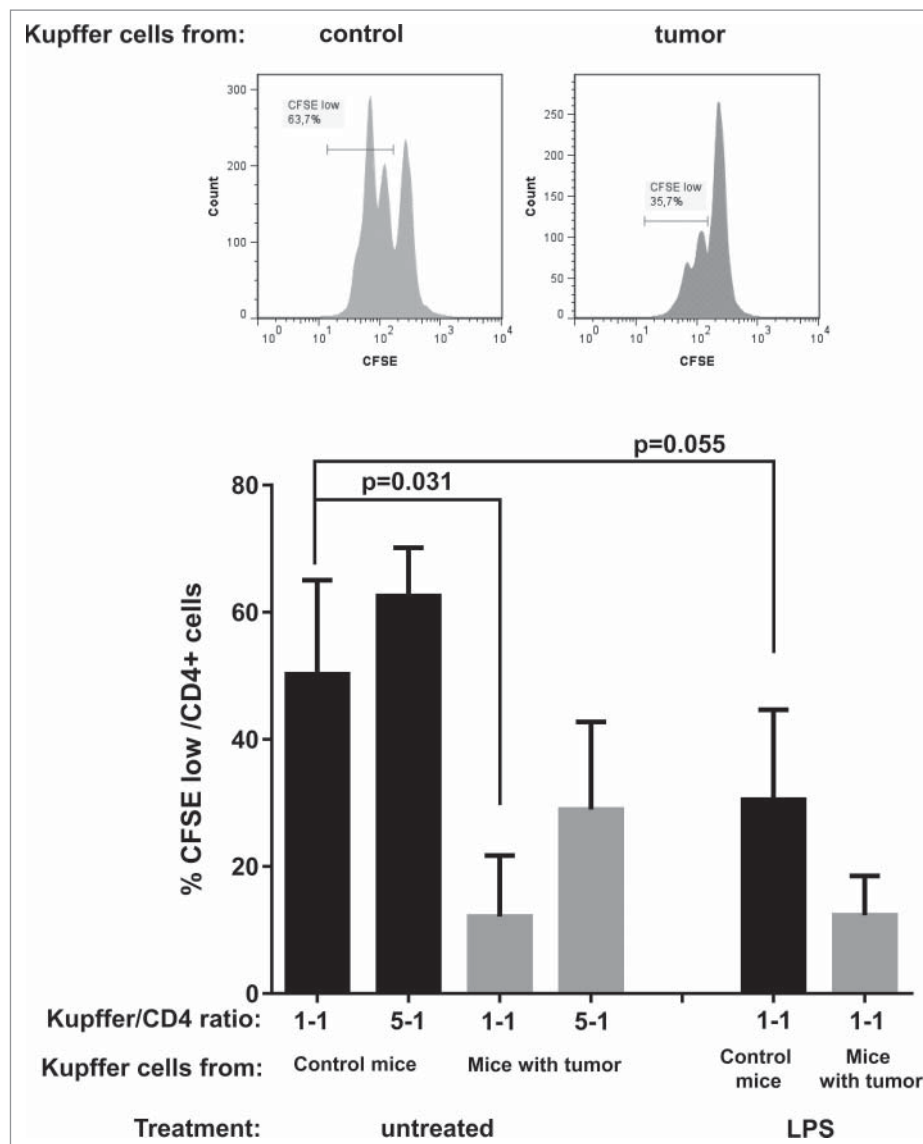


**Figure 2.** Antigen presentation by Kupffer cells from the surrounding parenchyma of HCC-bearing mice. Sorted Kupffer cells from control or HCC-bearing mice were incubated with CFSE-labeled CD4<sup>+</sup> cells from OT-II mice, with ovalbumine<sup>323-339</sup> peptide, and with or without LPS. After a 48-h incubation, CD4<sup>+</sup> cells were gated and proliferating CFSE<sup>low</sup> cells were assessed (upper panel). Results were expressed as the percentage of CFSE<sup>low</sup> cells over total CD4<sup>+</sup> cells (lower panel).

Programmed Death-Ligand 1 (PD-L1)) was increased both in tumor tissue and surrounding parenchyma compared to control liver parenchyma (MFI: 290 and 370, respectively, compared to 223 in controls). This distinct phenotype was more pronounced when the tumor diameter was greater than 0.5 cm. The capacity of Kupffer cells to present antigen was also assessed (Fig. 1B). Membrane MHCII expression was decreased on Kupffer cells from the tumor surrounding parenchyma compared to cells from control liver (MFI: 108 vs. 529).

#### **Kupffer cells from HCC-bearing animals have a decreased antigen-presenting activity**

Kupffer cells have an important role as antigen-presenting cells, and their efficiency for that purpose is related to the presence of co-stimulatory molecules.<sup>4</sup> To determine whether the observed co-stimulatory phenotype was related to cell functionality, Kupffer cells from control and HCC-bearing mouse livers were incubated with CFSE-labeled CD4<sup>+</sup> T cells from OT-II mice

(Fig. 2). This antigen-presentation assay revealed a decreased proliferation of CD4<sup>+</sup> T cells upon antigen presentation by Kupffer cells from HCC-bearing livers as compared to controls (ratio 1-1: 50.23% proliferation using Kupffer cells from controls versus 12.1% using Kupffer cells from HCC-bearing animals). Of note, a 3-h pre-incubation with lipopolysaccharide (LPS) decreased the ability of Kupffer cells to stimulate the antigen-specific proliferation of CD4<sup>+</sup> T cells. This observation is in line with previous data, and is associated to the ability of Kupffer cells (as some other tissue macrophages<sup>22</sup>) to release IL-10 and prostaglandin with a unique increase of CD274 expression under LPS stimulation (<sup>4,23</sup> and data not shown).

#### **MDSCs are increased in blood, spleen, liver, and tumor tissue of HCC-bearing mice**

MDSCs, described in mouse as CD45<sup>+</sup> CD11b<sup>+</sup> Gr1<sup>+</sup> cells, were characterized by flow cytometry in several compartments of HCC-bearing versus sham-operated mice (Fig. 3A). On day

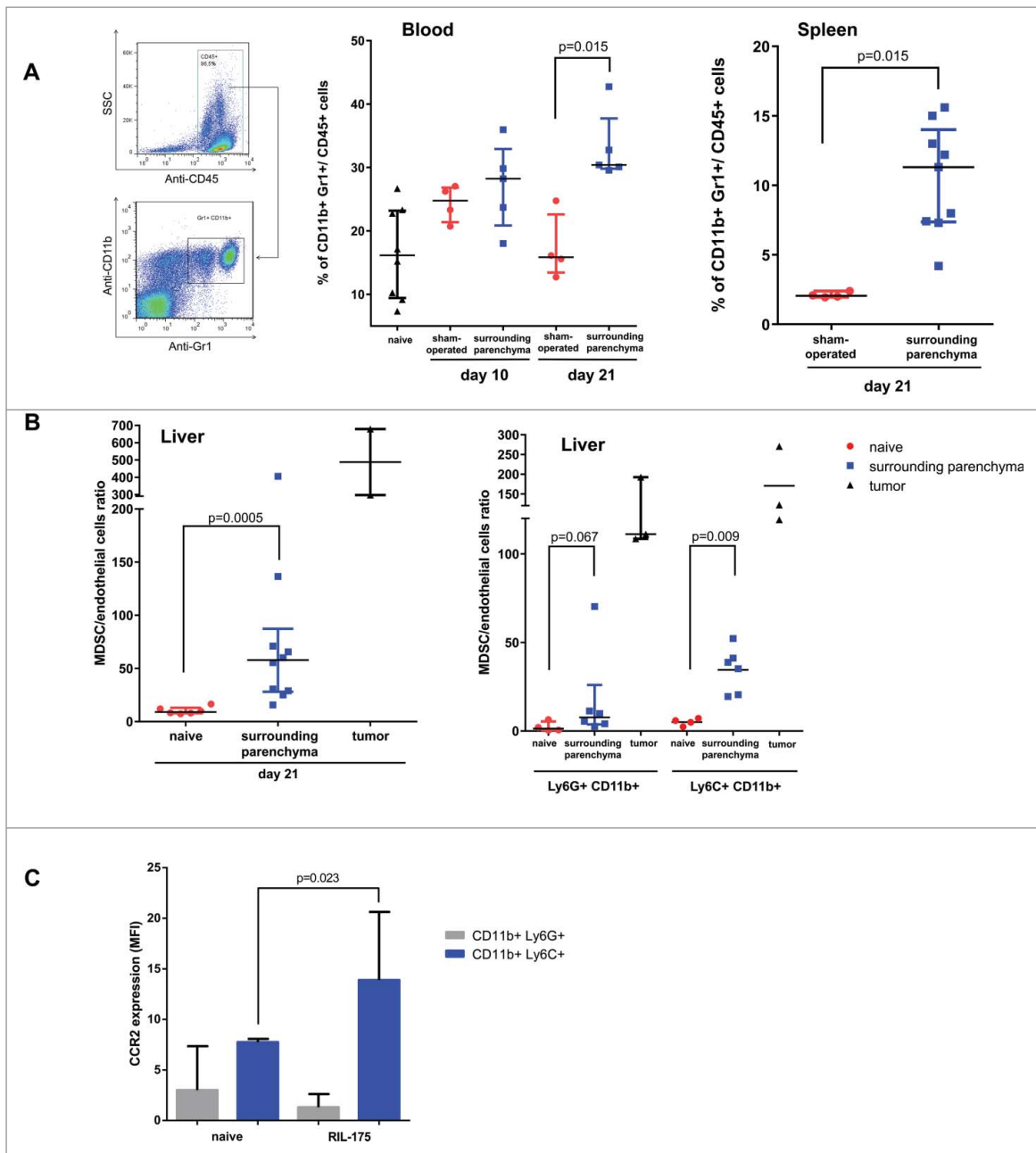


**Figure 3.** MDSC distribution in the blood, spleen and liver of HCC-bearing mice. (A) MDSCs, defined as CD45<sup>+</sup> CD11b<sup>+</sup> Gr1<sup>+</sup> cells, were assessed by flow cytometry in the blood of HCC-bearing versus control mice on day 10 and 21, and in the spleen on day 21. (B) The number of infiltrating MDSCs was assessed in the liver of control and HCC-bearing mice and in the tumor tissue (ratio MDSC/endothelial cells) (left panel). Granuloctytic (Ly6G<sup>+</sup> CD11b<sup>+</sup>) and monocytic (Ly6C<sup>+</sup> CD11b<sup>+</sup>) MDSC subsets were assessed in the liver of control and HCC-bearing mice and in the tumor tissue (ratio MDSC/endothelial cells) (right panel). (C) CCR2 expression level on granuloctytic and monocytic MDSCs isolated from the liver of control and from the surrounding parenchyma of HCC-bearing animals (MFI).

10 after laparotomy, the frequency of blood CD11b<sup>+</sup> Gr1<sup>+</sup> cells was increased in both HCC-bearing and control mice, which is likely linked to the surgical inflammation (Fig. 3A, middle). However, on day 21, CD11b<sup>+</sup> Gr1<sup>+</sup> cells further increased only in HCC-bearing mice (30% vs. 16% in HCC vs. mice undergoing sham laparotomy,  $p = 0.015$ ), and this time-point was used for further experiments. On day 21, CD11b<sup>+</sup> Gr1<sup>+</sup> cells were also increased in the spleen of HCC-bearing mice compared to sham-operated mice (11% and 2%, respectively,  $p = 0.015$ ) (Fig. 3A, right). Of note, the frequency of CD11b<sup>+</sup> Gr1<sup>+</sup> cells was similarly increased in other liver cancer models, including BNL-h1 HCC cells in BALB/c mice, and MC38 colo-rectal

metastasis cells in C57BL/6 mice (data not shown). In the liver, the number of infiltrating CD11b<sup>+</sup> Gr1<sup>+</sup> cells was increasing from control liver parenchyma (9.1 MDSC: 1 endothelial cell) to underlying liver parenchyma (57.85 MDSC: 1 endothelial cell) and to tumor tissue (487 MDSC: 1 endothelial cell),  $p < 0.001$  (Fig. 3B left). Both granuloctytic (Ly6G<sup>+</sup>) and monocytic (Ly6C<sup>+</sup>) MDSC populations were expanded with a similar pattern in naive, surrounding, and tumor parenchyma, respectively (Fig. 3B right).

HCC nodules have been shown to secrete CCL2 (MCP-1), a cytokine which can promote monocytic MDSC infiltration.<sup>18</sup> Thus, we measured MDSC surface expression of CCR2, the

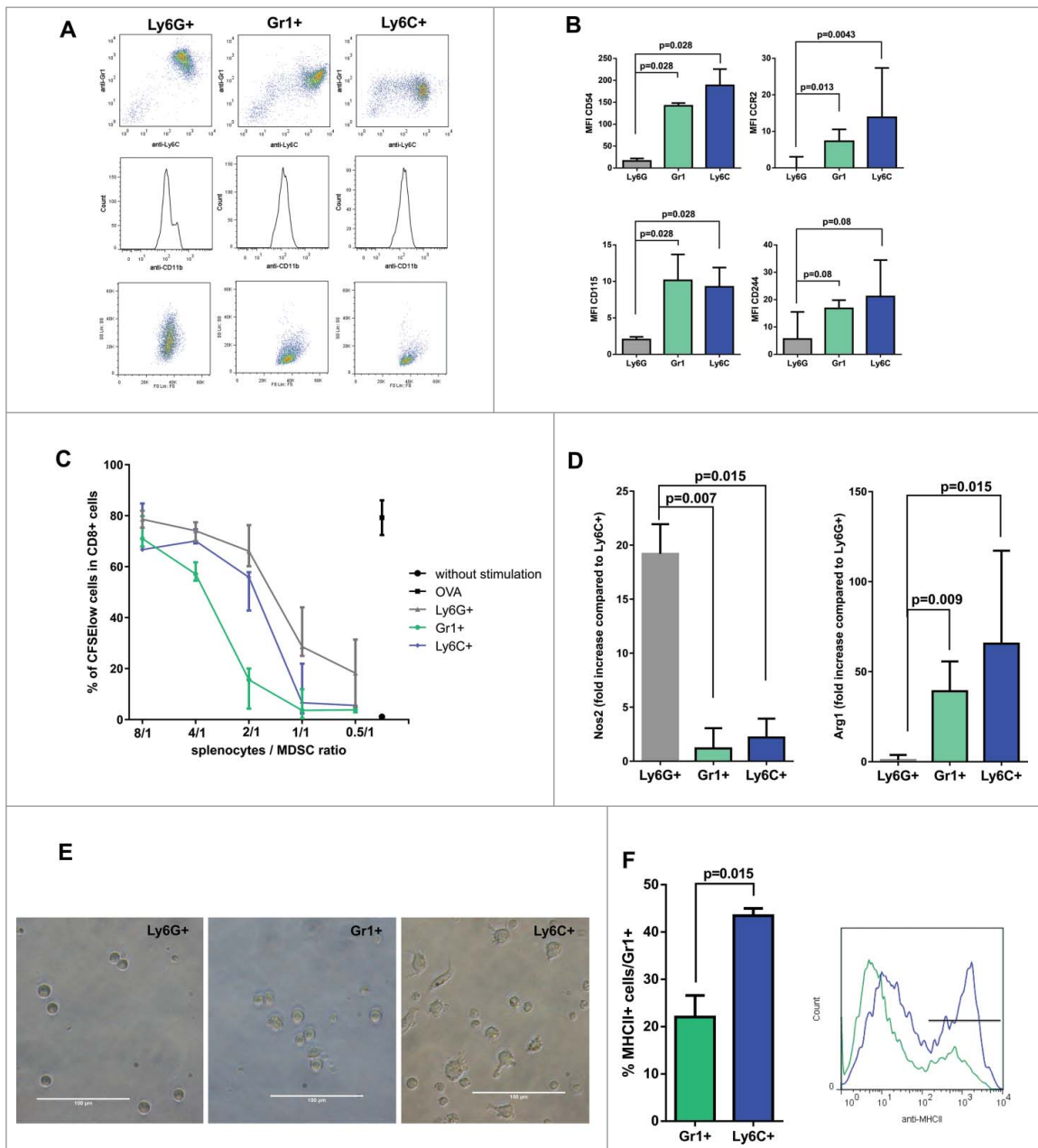


**Figure 4.** Identification of three MDSC subsets in HCC-bearing mice. (A) Flow cytometry profile of magnetically sorted Ly6G<sup>+</sup>, Gr1<sup>+</sup>, and Ly6C<sup>+</sup> cell subsets of MDSCs. (B) Phenotypes of the three CD11b-expressing populations were assessed according to the membrane markers reported in the literature (MFI of CCR2, CD244, CD54, and CD115). (C) Sorted MDSC subsets were incubated with CFSE-labeled splenocytes from OT-I mice at different splenocyte/MDSC ratio and the ovalbumine<sup>257-264</sup> peptide. After a 48-h incubation, CD8<sup>+</sup> cells were gated and CFSE<sup>low</sup> cells were assessed. Results were expressed as the percentage of proliferating CFSE<sup>low</sup> cells over total CD8<sup>+</sup> cells. (D) The expression levels of *Nos2* and *Arg1* were assessed by qPCR on FACS sorted-MDSC subsets ( $2^{-\Delta\Delta CT}$ , fold increase compared to one cell subset). (E) Morphology of sorted-MDSC subsets after a 12-h plating ( $\times 40$ , white bar 100  $\mu\text{m}$ ). (F) Sorted MDSC subsets were incubated with LPS. After a 24-h incubation, Gr1<sup>+</sup> cells were gated and MHCII<sup>+</sup> cells were assessed.

receptor for CCL2, and showed that it was more expressed on liver monocytic MDSC of HCC-bearing compared to sham-operated mice (MFI: 13.8 vs. 7.7,  $p = 0.023$  Fig. 3C).

### HCC-bearing mice demonstrate three MDSC subsets

In order to better study the subsets of MDSC in HCC-bearing mice, we magnetically sorted splenic MDSC at day 21. Unlike classically described,<sup>12</sup> not two, but three cell subsets expressing CD11b were isolated with various size, granularity, and levels of Ly6G and Ly6C molecules (Fig. 4A). For clarity purposes,

each cell subset is further referred according to the name of the antigen used to sort it (Ly6G<sup>+</sup>, Gr1<sup>+</sup>, and Ly6C<sup>+</sup>).

The phenotype of the three CD11b-expressing populations was assessed according to the MDSC surface markers reported in the literature (Fig. 4B).<sup>14,23</sup> Ly6C<sup>+</sup> and Gr1<sup>+</sup> cell subsets demonstrated an increased expression level of CCR2 (MCP-1 receptor), CD244 (2B4), and CD115 (M-CSFR). Unlike previous publications, we only observed a weak expression of CD244 and CD115 at the surface of Ly6G<sup>+</sup> cells.<sup>24</sup> These molecules were more expressed at the surface of Gr1<sup>+</sup> and Ly6C<sup>+</sup> subsets (Fig. 4B). CD54 was widely expressed at the surface of

both Gr1<sup>+</sup> and Ly6C<sup>+</sup> cell subsets, as previously described on monocytic MDSCs.<sup>25</sup>

Next, we examined the suppressive effect of these three CD11b-expressing cell subsets in an antigen-specific T cell proliferation assay with OT-I splenocytes (Fig. 4C). The three cell subsets adequately suppressed antigen-specific T cell proliferation (proliferation: 28.6%, 3.6%, and 6.5%, respectively, at splenocytes/MDSC ratio 1/1, compared to positive control: 79.2%). In addition, similar observations were made in other liver cancer models, including BNL-h1 HCC cells in BALB/c mice, and MC38 colo-rectal metastasis cells in C57BL/6 mice (data not shown). Finally, the three MDSC subsets were also detected in the liver, with a higher expression of CD54 in the Ly6C<sup>+</sup> cell subset than in the Gr1<sup>+</sup> cell subset. The three MDSC subsets sorted from the liver suppressed T cell proliferation (Fig. S1).

Furthermore, we assessed the expression levels of *Nos2* and *Arg1*, two genes involved in the L-Arginine metabolism and considered to mediate the suppressive activity of MDSCs.<sup>26</sup> *Nos2* was highly expressed in Ly6G<sup>+</sup> cells, whereas its expression remained lower in Gr1<sup>+</sup> ( $p = 0.007$ ) and Ly6C<sup>+</sup> ( $p = 0.015$ ) cells (fold increase: 19.19, 1.18, and 2.19, respectively) (Fig. 4D). In contrast, *Arg1* was more expressed in Gr1<sup>+</sup> ( $p = 0.009$ ) and Ly6C<sup>+</sup> ( $p = 0.015$ ) cells compared to Ly6G<sup>+</sup> cells (fold increase: 39.19, 65.57, and 0.95, respectively).

The three MDSC cell subsets showed distinct morphologies after a 12 h plating (Fig. 4E). Ly6G<sup>+</sup> and Gr1<sup>+</sup> cells kept a round shape with only rare plastic adhesion. Ly6C<sup>+</sup> cells developed more pseudopoda and adherences leading to a more differentiated morphology. Finally, a higher number of Ly6C<sup>+</sup> cells than Gr1<sup>+</sup> cells acquired the MHCII expression after a 24 h incubation with LPS (22% in Gr1<sup>+</sup> vs. 43.3% in Ly6C<sup>+</sup>) (Fig. 4F).

### Impact of MDSCs on Kupffer cells

MDSCs have demonstrated their suppressive activities on T cells, NK cells, and monocytes, but their effect on Kupffer cells has not been explored thus far.<sup>13-15</sup> Although Kupffer cells are not primarily secreting cells, they are still able to mount pro- and anti-inflammatory responses. Therefore, Kupffer cells were cultured with or without MDSC for 24 h (Fig. 5A) and ELISA assessments were performed on the culture media. LPS-induced CCL2 secretion was decreased when Kupffer cells were cultured with Gr1<sup>+</sup> and Ly6C<sup>+</sup> cells (1754 pg/mL vs. 1272 pg/mL ( $p = 0.03$ ) and 1283 pg/mL ( $p = 0.03$ ), respectively). Considering these two MDSC populations expressed CCR2, the receptor for CCL2, one should consider that at least part of this reduced CCL2 level is caused by MDSCs capturing CCL2 produced by Kupffer cells.

IL-18 secretion decreased when Kupffer cells were cultured with the Ly6G<sup>+</sup> and Ly6C<sup>+</sup> cells (70.8 pg/mL compared to 56.5 pg/mL ( $p = 0.044$ ) and 56.3 pg/mL ( $p = 0.028$ ), respectively), but not after incubation with Gr1<sup>+</sup> cells. Of note, Gr1<sup>+</sup> cells alone were able to secrete IL-18, and only a weak secretion of IL-18 was detected both in unstimulated and stimulated Kupffer cells. IL-10 levels were increased when Kupffer cells were cultured with the three MDSC subsets, but only

incubation with Ly6C<sup>+</sup> cells reached significance (365 pg/mL vs. 549 pg/mL,  $p = 0.021$ ).

IL-1 $\beta$  production was increased after incubation with Gr1<sup>+</sup> and Ly6C<sup>+</sup> cells (205 pg/mL compared to 320 pg/mL,  $p = 0.017$ , and 362 pg/mL,  $p = 0.0043$ ). IL-6 production was unchanged after incubation with the three MDSC subsets. Of note, MDSC subsets were also able to secrete IL-10, IL-6, and IL-1 $\beta$  and the added levels of secretion by Kupffer cells alone and MDSCs alone were lower than the combined level of secretion, suggesting a potential inhibitory effect of MDSCs.

Thanks to their phagocytic activity, Kupffer cells are considered to constitute the first line of defense against circulating tumor cells, pathogens, and non-self particles in the liver. Thus, using dextran particles phagocytosis assay, we evaluated Kupffer cell endocytosis capacity after 24 h of incubation with MDSCs. As shown in Fig. 5B, MDSCs did not impact significantly on the endocytosis of dextran molecules by Kupffer cells.

To determine the phenotype of Kupffer cells as antigen-presenting cells upon modulation by MDSCs, we measured the expression of co-stimulatory molecules after incubation with the three MDSC subsets. Kupffer cells demonstrated an increased expression of the inhibitory CD274 (PD-L1) after incubation with the three MDSC populations (MFI: 439 vs. 620, 632 and 555 for Ly6G<sup>+</sup>, Gr1<sup>+</sup> and Ly6C<sup>+</sup>, respectively). CD86 expression was also increased in the presence of Ly6G<sup>+</sup>, Gr1<sup>+</sup>, and Ly6C<sup>+</sup> MDSC (MFI: 201 vs. 284, 268 and 258 for Ly6G<sup>+</sup>, Gr1<sup>+</sup> and Ly6C<sup>+</sup>, respectively) (Fig. 6A). Membrane MHCII expression was increased on Kupffer cells after incubation with MDSC populations (MHCII MFI (355 vs. 541, 491 and for Ly6G<sup>+</sup>, Gr1<sup>+</sup>, and Ly6C<sup>+</sup>, respectively).

Finally, to determine the impact of MDSCs on Kupffer cell function as antigen-presenting cells, we measured CD4<sup>+</sup> T cell proliferation in the presence of Kupffer cells previously incubated with the three MDSC subsets (Fig. 6B). Although MDSCs were only used for a pre-incubation of Kupffer cells (thus avoiding any direct inhibitory MDSC-CD4<sup>+</sup> T cell effect), a decreased CD4<sup>+</sup> proliferation was observed with all MDSC subsets (45.9% vs. 35.3%, 26.5%, and 32.1% for Ly6G<sup>+</sup>, Gr1<sup>+</sup>, and Ly6C<sup>+</sup>, Fig. 6B). In order to address the potential interactions between Kupffer cells and T cells, anti-PD-L1 and anti-IL-10 antibodies and COX-2 inhibitor (CAY10404) were added. No statistically significant differences T cell proliferation were detected.

### Discussion

The present study demonstrates that the immune changes provoked by mouse liver cancer lead (1) to a decreased antigen-presentation activity of Kupffer cells (related to a decreased level of CD86 and MHCII and an increased level of CD274), (2) to the expansion of three MDSC subsets with specific phenotype and function, and (3) to the modulation of co-stimulatory/co-inhibitory molecules on Kupffer cells via all three MDSC subtypes.

Kupffer cells are key players in the clearance of tumor cells. They have the capacity to clear mouse circulating tumor cells after administration of anti-EGFR antibody,<sup>2</sup> and their activation by LPS prevents tumor growth.<sup>27</sup> Conversely, their depletion at the time of tumor cell implantation promotes colon

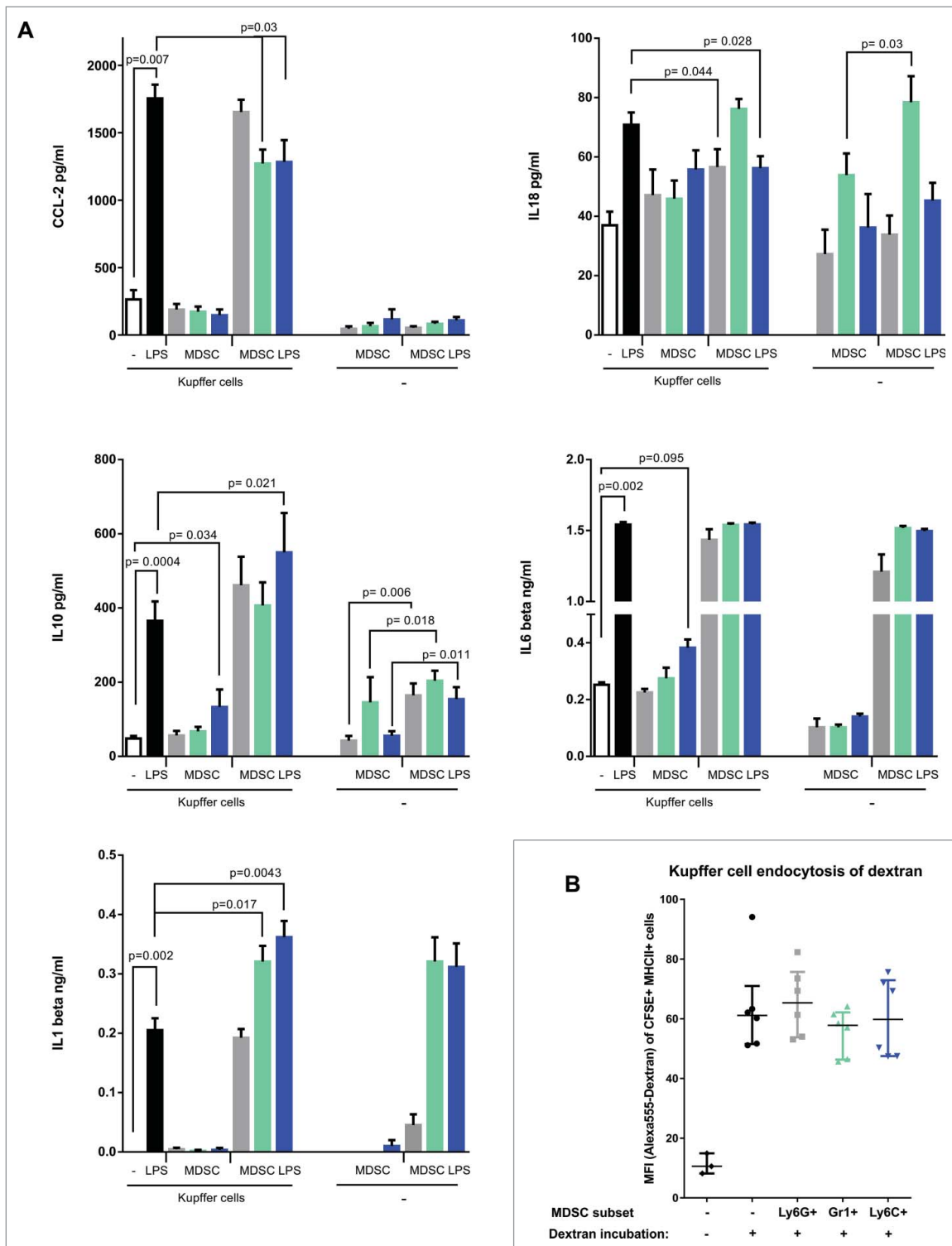


**Figure 5.** Kupffer cell secretion and endocytosis after incubation with the MDSC subsets. CFSE-labeled Kupffer cells from naive mice were incubated with or without MDSC subsets and with or without LPS for 24 h. (A) ELISA were performed to detect CCL2, IL-10, IL-18, IL-6, and IL-1 $\beta$  in supernatants (pg/mL). (B) Endocytosis was assessed by exposing Kupffer cells to Alexa555-Dextran for a 4-h incubation. Endocytosis was measured by flow cytometry as the Alexa555 MFI on CFSE<sup>+</sup> MHCII<sup>+</sup> Kupffer cells population.

cancer metastases.<sup>28,29</sup> Kupffer cells have commonly been explored as pro-inflammatory, pro-fibrogenic, and pro-carcinogenic stakeholders in the context of HCC, mainly looking at the secretion of IL-6, IL-1 $\beta$ , and epidermal growth factor.<sup>30,31</sup>

Here, we designed a unique Kupffer cell sorting strategy, which yields a highly homogeneous Kupffer cell population, by

specifically excluding circulating macrophages and Kupffer cell/endothelial cell doublets (Fig. 1A). This point is of crucial importance, as contaminating circulating macrophages could alter the observed phenotype. For instance, the balance of mediators favoring inflammation, tissue scarring or remodeling can be shifted by subtle differences in the populations of

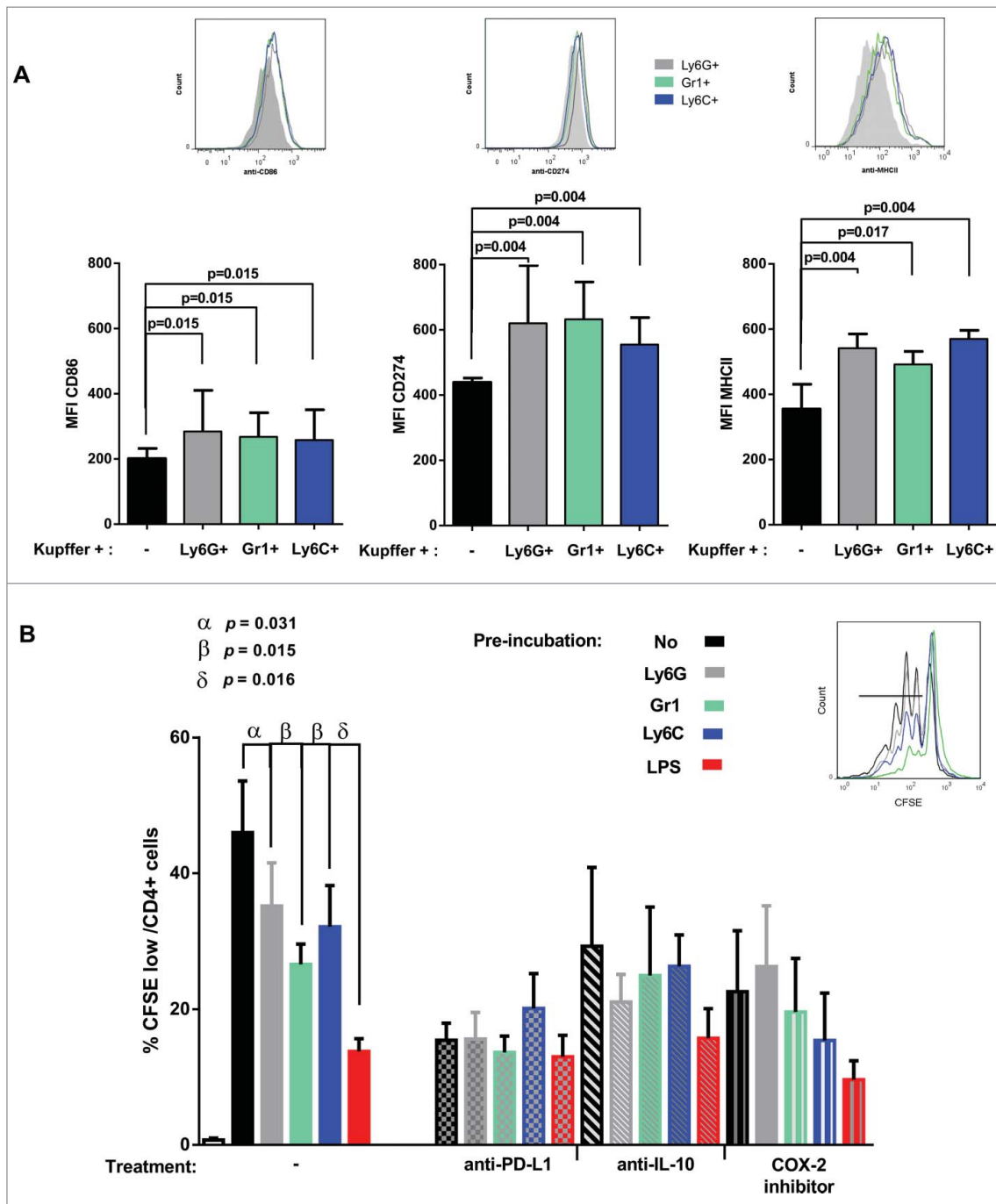


**Figure 6.** Impact of MDSC subsets on Kupffer cells co-stimulatory molecule expression and antigen presentation. (A) CFSE-labeled Kupffer cells from naive mice were incubated with or without MDSC subsets for 24 h. Activation level was quantified by flow cytometry as the MFI of CD86, CD274 (PD-L1), and MHCII on CFSE<sup>+</sup> MHCII<sup>+</sup> Kupffer cells population. (B) Kupffer cells from naive mice were incubated with sorted MDSC subsets. After a 24 h-incubation, MDSCs were removed and CFSE-labeled CD4<sup>+</sup> cells from OT-II mice were added with anti-PD-L1 or anti IL-10 antibodies or COX-2-inhibitor. After a further 48-h incubation, CD4<sup>+</sup> cells were gated and proliferating CFSE<sup>low</sup> cells were assessed. Results were expressed as the percentage of CFSE<sup>low</sup> cells over total CD4<sup>+</sup> cells.

monocytes recruited to the liver, with monocyte-derived Ly6C<sup>high</sup> F4-80<sup>int</sup> macrophages being associated with liver fibrosis, and monocyte-derived Ly6C<sup>int</sup> F4-80<sup>int</sup> macrophages having anti-fibrotic activities.<sup>32,33</sup>

Taking advantage of this homogeneous well-defined population, we demonstrate that, in the presence of HCC, Kupffer cells have a decreased Ag-presentation activity, which is linked to decreased expression of co-stimulatory CD86 and MHCII molecules and an increased level of co-inhibitory CD274. This observation is associated with HCC

size, and can explain why HCC cells are able to escape Kupffer cell surveillance.

In an effort to better understand the decreased Ag-presentation by Kupffer cells in the context of HCC, their interaction with MDSCs was further explored. These experiments were conducted with spleen MDSCs, as liver and spleen MDSCs both derive from bone marrow progenitors and have comparable phenotype and suppressive effects, as demonstrated herein and by others.<sup>34</sup> In addition, isolated liver MDSCs are less numerous and of lower purity (between 57% and 80%). For the



first time, three (and not two) distinct CD11b<sup>+</sup> cell subsets, with specific size, granularity, and expression level of Gr1, were isolated. Ly6G<sup>+</sup> cells demonstrated a classically described granulocytic phenotype, and lower expression levels of both CCR2 and CD54.<sup>14</sup> Unlike previously reported, they also demonstrated decreased levels of CD244 and CD115, but remained truly suppressive cells (Fig. 4C).<sup>24</sup> Of note, such different levels of expression of CD244 and CD115 compared to previously published data could be due to the heterogeneity of MDSC populations according to tumor type and localization.<sup>14</sup>

The third and new MDSC subset (described herein as Ly6C<sup>+</sup>) had been previously postulated in mouse models of subcutaneous tumors, but a further characterization had not been performed.<sup>35</sup> Ly6C<sup>+</sup> and Gr1<sup>+</sup> cells both show monocytic phenotypes and similar surface markers, but only Ly6C<sup>+</sup> cells are able to quickly evolve into macrophage-like cells, and express more membrane MHCII molecules after culture. Thus, we reasoned that Ly6C<sup>+</sup> may represent more differentiated cells (Figs. 4E and F) that derive from Gr1<sup>+</sup> cells after undergoing a maturation process with a lower ability to bind anti-Gr1 antibody (they remain in the flow-through after Gr1 selection, but can be positively selected based on Ly6). Unlike Ly6C<sup>+</sup> cells, Gr1<sup>+</sup> cells are able to secrete IL-18 after stimulation with LPS, but less IL-10, further supporting that Gr1<sup>+</sup> cells harbor a higher plasticity potential, and that Ly6C<sup>+</sup> cells are already differentiated into tumor-associated macrophages, or M2-like macrophages with a lesser inflammatory profile.

All MDSC subsets demonstrated potent suppressive activities on T cells, which is in line with their postulated function of modulatory suppressor cells. Their action on Kupffer cells had never been explored thus far, and our novel findings indicate that they are able to alter various cytokine secretion profiles (Fig. 5), without showing a significant impact on Kupffer cell endocytosis. Moreover, MDSCs can foster the expression of both CD274 (PD-L1), which had already been suggested when looking at circulating macrophages,<sup>34</sup> and CD86 and MHCII, which is a new observation. This increase in CD86 expression could be related to the known mode of action of MDSCs: MDSC suppress T cell activation mainly through the depletion of L-arginine in the micro-environment, but also by producing reactive oxygen species (ROS).<sup>36-38</sup> MDSC-mediated ROS production has been shown to increase Kupffer cell expression of CD80, another co-stimulatory molecule acting in tandem with CD86 to prime T cells.<sup>11</sup> This could explain the increase in CD86 on Kupffer cells, and potentially also of CD274. Overall, we propose that, in the presence of HCC, MDSC recruitment alters both Kupffer cell co-stimulatory and co-inhibitory functions, which imbalance results in a decreased antigen-presenting capacity of resident liver macrophages (Fig. 2, Fig. 6B). On T cells, the engagement of programmed death-1 (PD-1) by CD274 during antigen recognition induces the cross-linkage of the antigen-receptor complex with PD-1. This results in the inhibition of T cell activation, which also depends on others co-stimulatory signals like CD86/CD28 linkage.<sup>39,40</sup> This hypothesis is, however, not in line with the increased MHCII expression on Kupffer cells after *in vitro* incubation with MDSC (Fig. 6A). The phenotype of Kupffer cells after incubation with MDSC is different from the one observed *ex vivo* on Kupffer cells from the tumor-surrounding parenchyma

(Figs. 6A and 1B). The presence of tumor cells *in vivo* and their direct impact on Kupffer cells might be an explanation of this difference and should better reflect reality.

The present study is limited by the lack of experiments assessing the impact of MDSCs on Kupffer cells *in vivo*. Until recently, such experiments were not possible due to the lack of efficient and specific strategy to deplete MDSCs, especially in the liver.<sup>41</sup> For instance, the use of anti-Gr1 antibody failed to clear MDSCs, and the use of drugs, such as 5-fluorouracil, only marginally decreased their level due to other homeostatic mechanisms.<sup>42,43</sup> However, a recent work depleting MDSCs through the use of peptibodies led to a decreased tumor growth.<sup>44,45</sup> Overall, MDSCs have a clear impact on cancer growth, where their effect on Kupffer cells is one of the mechanisms.

In summary, the current study reports, for the first time, three subsets of MDSCs in mouse livers with HCC. Our findings suggest that MDSCs and Kupffer cells undergo phenotypic and functional changes in the presence of HCC. The observed suppressive effects of MDSCs on Kupffer cells deserve further attention, with the aim to improve the management of patients with HCC.

## Materials and methods

### Animals and HCC induction

All experiments were performed under an experimental protocol approved by the ethical committee of the University of Geneva, and by the Geneva veterinary authorities (authorization n°GE/56/15). Male C57BL/6 mice (8 weeks) were purchased from Janvier. Male OT-I mice and OT-II mice were purchased from Charles River. They were housed under 12/12-h light/dark cycles, with food and water *ad libitum*. Four hundred thousand RIL-175 HCC cells (kindly provided by Prof. T. Greten, NIH) were prepared in 50  $\mu$ L sterile Phosphate Buffer Saline, and gently injected underneath the liver capsule of the median lobe with a 29G needle. For selected experiments, BNL-h1 HCC cells were injected in BALB/c mice, and MC38 colo-rectal metastasis cells in C57BL/6 mice.<sup>46</sup> Successful inoculation was confirmed by the absence of bleeding and by the visualization of a local liver discoloration. At relevant time-points, the median lobe (with the tumor nodule) was removed and MDSCs were isolated from the other lobes.

### Liver cell isolation

The liver was perfused *in vivo* for 5 min using retrograde perfusion through the right atrium with a Wash Solution in order to remove red blood cells (HBSS, EGTA 0.5 mM, HEPES 25 mM, Penicillin-Streptomycin 1  $\mu$ g/mL, Glucose 0.1%, and Heparin 5 U/mL). Liver Digest Medium was subsequently perfused at 5 mL/min for 5 min at 37°C (IMDM, Collagenase IV, Worthington at 0.5 mg/mL, and DNase I, Roche at 0.1 mg/mL). The liver was manually cut into 1 mm pieces in 4°C DMEM with 10% Fetal Bovine Serum (Gibco), and crushed through a cell strainer (70  $\mu$ m). The single-cell suspension was centrifuged twice at 68 g for 5 min at 4°C to remove hepatocytes. Non-parenchymal cells were purified using centrifugation at

1,400 g for 30 min in an 8.2/17.6% Optiprep gradient, without acceleration nor brake. Cells at the interface were collected and counted. For specific experiments, Kupffer cells were isolated after 15-min incubation with anti-CD11b-microbeads (Miltenyi Biotec), and positive magnetic sorting using LS MACS columns (Miltenyi Biotec). For antigen-presenting cell assay, Optiprep-purified cells were sorted on a BioRad S3 cell Sorter after a F4-80/I-A-I-E (mouse MHC class II) labeling.

### MDSC isolation

Tumor-bearing animals were sacrificed 3 weeks after cancer cell injection. The spleen was removed and crushed through a cell strainer. Splenocytes were purified in a Ficoll density gradient. Isolated cells were washed and counted in view of a magnetic separation with the Myeloid-Derived Suppressor Cell Isolation Kit (Miltenyi Biotec). The first two cell subsets (Ly6G<sup>+</sup> and Gr1<sup>+</sup>) were purified according to manufacturer's instructions. Briefly, splenocytes were incubated with biotin anti-Ly6G antibodies, and subsequently with magnetic beads conjugated to anti-biotin antibodies. The flow-through was centrifuged and incubated with biotin anti-Gr1 antibodies, and subsequently incubated with magnetic beads conjugated to streptavidin. The negative fraction was incubated with anti-Ly6C Ab (HK-1.4, Biolegend) and anti-rat IgG microbeads (Miltenyi Biotec). All cell subsets were isolated on AutoMACS Pro device (Miltenyi Biotec), with purities of >95%, >80%, and >78% for Ly6G, Gr1, and Ly6C. For gene expression experiments, cell purification was further improved with PE anti-Ly6C Ab, and FITC anti-Gr1 Ab labeling, and through a flow analyzer cell-sorter MoFlo Astrios (Beckman Coulter).

### Flow cytometry analysis

Cells were incubated with Fc-blocking reagent (TrueStain, Biolegend) for 5 min, and subsequently stained for 20 min at 4°C with the relevant antibody. Some antibodies were used to analyze Kupffer cells: FITC anti-F4-80 (BM8), APC anti-I-A-I-E (M5/114.15.2), PE anti-CD86 (GL-1), PECy7 anti-CD68 (FA-11), PerCP anti-CD11b (M1/70) (Biolegend), PE anti-CD273 (122), and anti-CD274 (MIH5) (eBiosciences). For experiments involving Kupffer cell/MDSC co-culture, Kupffer cells were first labeled with CFSE (0.5  $\mu$ M, Invitrogen). MDSC were characterized with the following antibodies: APC anti-CCR2 (475301, R&D Systems), APC anti-CD244.2 (eBio244F4, eBiosciences), APC anti-CD54 (YN1/1.7.4), APC anti-CD115 (AFS98), PE anti-Ly6C (HK1.4), PerCP anti-CD11b (M1/70), Alexa-Fluor488 anti-CD146 (ME-9F1), PECy7 anti-Gr1 (RB6-8C5), APC Cy7 anti-CD45 (30-F11, Biolegend). All samples were acquired with a Flow Cytometer Cyan (Beckman Coulter), and analyzed with FloJo (Treestar).

### Real-time polymerase chain reaction (qPCR)

Cells were lysed in TRIzol<sup>®</sup> Reagent (Life Technologies) and total RNA was purified using the RNeasy Micro Kit (Qiagen), according to the manufacturer's instructions. cDNA was synthesized by extending a mix of random primers with the High Capacity cDNA Reverse Transcription Kit in the presence of

RNase Inhibitor (Applied Biosystems). The relative quantity of each transcript was normalized according to the expression of *rplp1*. Primer sequences are available upon request. Amplification reactions were performed in a total volume of 20  $\mu$ L using a Thermocycler sequence detector (BioRad CFX96) with qPCR Core kit for SYBR Green I (Eurogentec).

### ELISA

Supernatant cytokines were quantified using ELISA kits for mouse CCL2, IL-10, IL-1 $\beta$ , and IL-18 (eBiosciences).

### Suppression assay

CFSE-labeled splenocytes from OT-I mice were incubated with or without MDSCs in RPMI supplemented with ovalbumin<sup>257-264</sup> peptide (SIINFEKL, 0.2  $\mu$ g/mL, Sigma-Aldrich). After 3 d, cells were labeled with PE anti-CD8 Ab (53-6.7) and APC-Cy7 anti-TCR Ab (H57-597) (Biolegend).

### Antigen-presenting cell assay

FACS-sorted Kupffer cells from control or HCC-bearing mice were cultured in 96-well plates overnight. Splenocytes and lymph node cells from OT-II mice were labeled with CFSE (0.5  $\mu$ M). CD4<sup>+</sup> T cells were purified using a CD4<sup>+</sup> T Cell Isolation Kit (Miltenyi Biotec). After 3-h-incubation with ovalbumin<sup>323-339</sup> peptide (ISQAVHAAHAEINEAGR, 40 ng/mL, Sigma-Aldrich) with or without LPS (400 ng/mL, Sigma-Aldrich), CFSE-labeled CD4<sup>+</sup> cells were added to each well at different Kupffer cells/CD4<sup>+</sup> cells ratio. For selected experiments anti-PD-L1 (10F.9G2), anti-IL-10 (JES5-16E3) (Biolegend), and CAY10404 (Cayman Chemical) were added.

### Statistical analysis

All data are expressed as median  $\pm$  interquartile, unless otherwise specified. Non-parametric Mann-Whitney U test or Wilcoxon matched-pair tests were used, where appropriate. Statistical analyses were performed using the package Prism (Graphpad). All p-values are two-tailed and significance was set at the 5% level.

### Disclosure of potential conflicts of interest

No potential conflicts of interest were disclosed.

### Acknowledgments

The authors are grateful to Ms Cécile Gameiro and M Jean-Pierre Aubry from the flow cytometry core facilities for their excellent technical assistance.

### Funding

The project was supported by grants from the Swiss National Science Foundation (PP00P3\_139021, 310030\_138341), the Artères foundation, the Geneva Cancer League, and the Geneva Academic Society.

## ORCID

Vaihere Delaune  <http://orcid.org/0000-0001-8931-0977>

## References

- Thomson AW, Knolle PA. Antigen-presenting cell function in the tolerogenic liver environment. *Nat Rev Immunol* 2010; 10:753-66; PMID:20972472; <http://dx.doi.org/10.1038/nri2858>
- Gül N, Babes L, Siegmund K, Korthouwer R, Bögels M, Braster R, Vidarsson G, ten Hagen TLM, Kubes P, van Egmond M. Macrophages eliminate circulating tumor cells after monoclonal antibody therapy. *J Clin Invest* 2014; 124:812-23; PMID:24430180; <http://dx.doi.org/10.1172/JCI66776>
- You Q, Cheng L, Kedl RM, Ju C. Mechanism of T cell tolerance induction by murine hepatic kupffer cells. *Hepatology* 2008; 48:978-90; PMID:18712788; <http://dx.doi.org/10.1002/hep.22395>
- Crispe IN. Liver antigen-presenting cells. *J Hepatol* 2011; 54:357-65; PMID:21084131; <http://dx.doi.org/10.1016/j.jhep.2010.10.005>
- Li M, Sun R, Xu L, Yin W, Chen Y, Zheng X, Lian Z, Wei H, Tian Z. Kupffer cells support hepatitis B virus-mediated CD8<sup>+</sup> T cell exhaustion via hepatitis B core antigen-TLR2 interactions in mice. *J Immunol* 2015; 195:3100-9; PMID:26304988; <http://dx.doi.org/10.4049/jimmunol.1500839>
- Peralta C, Jiménez-Castro MB, Gracia-Sancho J. Hepatic ischemia and reperfusion injury: effects on the liver sinusoidal milieu. *J Hepatol* 2013; 59:1094-106; PMID:23811302; <http://dx.doi.org/10.1016/j.jhep.2013.06.017>
- Baffy G. Kupffer cells in non-alcoholic fatty liver disease: the emerging view. *J Hepatol* 2009; 51:212-23; PMID:19447517; <http://dx.doi.org/10.1016/j.jhep.2009.03.008>
- Strauss O, Dunbar PR, Bartlett A, Phillips A. The immunophenotype of antigen presenting cells of the mononuclear phagocyte system in normal human liver—a systematic review. *J Hepatol* 2015; 62:458-68; PMID:25315649; <http://dx.doi.org/10.1016/j.jhep.2014.10.006>
- Kinoshita M, Uchida T, Sato A, Nakashima M, Nakashima H, Shono S, Habu Y, Miyazaki H, Hiroi S, Seki S. Characterization of two F4/80-positive Kupffer cell subsets by their function and phenotype in mice. *J Hepatol* 2010; 53:903-10; PMID:20739085; <http://dx.doi.org/10.1016/j.jhep.2010.04.037>
- Klein I, Cornejo JC, Polakos NK, John B, Wuensch SA, Topham DJ, Pierce RH, Crispe IN. Kupffer cell heterogeneity: functional properties of bone marrow derived and sessile hepatic macrophages. *Blood* 2007; 110:4077-85; PMID:17690256; <http://dx.doi.org/10.1182/blood-2007-02-073841>
- Maemura K, Zheng Q, Wada T, Ozaki M, Takao S, Aikou T, Bulkeley GB, Klein AS, Sun Z. Reactive oxygen species are essential mediators in antigen presentation by Kupffer cells. *Immunol Cell Biol* 2005; 83:336-43; PMID:16033528; <http://dx.doi.org/10.1111/j.1440-1711.2005.01323.x>
- Talmadge JE, Gabrilovich DI. History of myeloid-derived suppressor cells. *Nat Rev Cancer* 2013; 13:739-52; PMID:24060865; <http://dx.doi.org/10.1038/nrc3581>
- Fortin C, Huang X, Yang Y. NK cell response to vaccinia virus is regulated by myeloid-derived suppressor cells. *J Immunol* 2012; 189:1843-9; PMID:22798671; <http://dx.doi.org/10.4049/jimmunol.1200584>
- Youn J-I, Nagaraj S, Collazo M, Gabrilovich DI. Subsets of myeloid-derived suppressor cells in tumor-bearing mice. *J Immunol* 2008; 181:5791-802; PMID:18832739; <http://dx.doi.org/10.4049/jimmunol.181.8.5791>
- Beury DW, Parker KH, Nyandjo M, Sinha P, Carter KA, Ostrand-Rosenberg S. Cross-talk among myeloid-derived suppressor cells, macrophages, and tumor cells impacts the inflammatory milieu of solid tumors. *J Leukoc Biol* 2014; 96:1109-18; PMID:25170116; <http://dx.doi.org/10.1189/jlb.3A0414-210R>
- Sinha P, Clements VK, Bunt SK, Albelda SM, Ostrand-Rosenberg S. Cross-talk between myeloid-derived suppressor cells and macrophages subverts tumor immunity toward a type 2 response. *J Immunol* 2007; 179:977-83; PMID:17617589; <http://dx.doi.org/10.4049/jimmunol.179.2.977>
- Schrader J. The role of MDSCs in hepatocellular carcinoma - in vivo veritas? *J Hepatol* 2013; 59:921-3; PMID:23958935; <http://dx.doi.org/10.1016/j.jhep.2013.08.003>
- Kapanadze T, Gamrekelashvili J, Ma C, Chan C, Zhao F, Hewitt S, Zender L, Kapoor V, Felsher DW, Manns MP et al. Regulation of accumulation and function of myeloid derived suppressor cells in different murine models of hepatocellular carcinoma. *J Hepatol* 2013; 59:1007-13; PMID:23796475; <http://dx.doi.org/10.1016/j.jhep.2013.06.010>
- Gottfried E, Kunz-Schughart LA, Weber A, Rehli M, Peuker A, Müller A, Kastenberger M, Brockhoff G, Andreesen R, Kreutz M. Expression of CD68 in non-myeloid cell types. *Scand J Immunol* 2008; 67:453-63; PMID:18405323; <http://dx.doi.org/10.1111/j.1365-3083.2008.02091.x>
- Tacke F, Zimmermann HW. Macrophage heterogeneity in liver injury and fibrosis. *J Hepatol* 2014; 60:1090-6; PMID:24412603; <http://dx.doi.org/10.1016/j.jhep.2013.12.025>
- Baeck C, Wei X, Bartneck M, Fecht V, Heymann F, Gassler N, Hittatiya K, Eulberg D, Luedde T, Trautwein C et al. Pharmacological inhibition of the chemokine C-C motif chemokine ligand 2 (monocyte chemoattractant protein 1) accelerates liver fibrosis regression by suppressing Ly-6C<sup>+</sup> macrophage infiltration in mice. *Hepatology* 2014; 59:1060-72; PMID:24481979; <http://dx.doi.org/10.1002/hep.26783>
- Chanteux H, Guisset AC, Pilette C, Sibille Y. LPS induces IL-10 production by human alveolar macrophages via MAPKs- and Spl-dependent mechanisms. *Respir Res* 2007; 8:71; PMID:17916230; <http://dx.doi.org/10.1186/1465-9921-8-71>
- Wiegand C, Frenzel C, Herkel J, Kallen K-J, Schmitt E, Lohse AW. Murine liver antigen presenting cells control suppressor activity of CD4<sup>+</sup>CD25<sup>+</sup> regulatory T cells. *Hepatology* 2005; 42:193-9; PMID:15962311; <http://dx.doi.org/10.1002/hep.20756>
- Youn J-I, Collazo M, Shalova IN, Biswas SK, Gabrilovich DI. Characterization of the nature of granulocytic myeloid-derived suppressor cells in tumor-bearing mice. *J Leukoc Biol* 2012; 91:167-81; PMID:21954284; <http://dx.doi.org/10.1189/jlb.0311177>
- Ostrand-Rosenberg S. Myeloid-derived suppressor cells: more mechanisms for inhibiting antitumor immunity. *Cancer Immunol Immunother* 2010; 59:1593-600; PMID:20414655; <http://dx.doi.org/10.1007/s00262-010-0855-8>
- Bronte V, Serafini P, Mazzoni A, Segal DM, Zanovello P. L-arginine metabolism in myeloid cells controls T-lymphocyte functions. *Trends Immunol* 2003; 24:301-5; PMID:19941314; [http://dx.doi.org/10.1016/S1471-4906\(03\)00132-7](http://dx.doi.org/10.1016/S1471-4906(03)00132-7)
- Chen GG, Lau WY, Lai PBS, Chun YS, Chak ECW, Leung BCS, Lam IKY, Lee JFY, Chui AKK. Activation of Kupffer cells inhibits tumor growth in a murine model system. *Int J Cancer* 2002; 99:713-20; PMID:12115505; <http://dx.doi.org/10.1002/ijc.10412>
- Bayon LG, Izquierdo MA, Sirovich I, Van Rooijen N, Beelen RH, Meijer S. Role of Kupffer cells in arresting circulating tumor cells and controlling metastatic growth in the liver. *Hepatology* 1996; 23:1224-31; PMID:8621157; <http://dx.doi.org/10.1002/hep.510230542>
- Schuurman B, Heuff G, Beelen RHJ, Meyer S. Enhanced human kupffer cell-mediated cytotoxicity after activation of the effector cells and modulation of the target cells by interferon- $\gamma$ : A mechanistic study at the cellular level. *Cell Immunol* 1995; 165:141-7; PMID:7671318; <http://dx.doi.org/10.1006/cimm.1995.1197>
- Wu J, Li J, Salcedo R, Mivechi NF, Trinchieri G, Horuzsko A. The proinflammatory myeloid cell receptor TREM-1 controls Kupffer cell activation and development of hepatocellular carcinoma. *Cancer Res* 2012; 72:3977-86; PMID:22719066; <http://dx.doi.org/10.1158/0008-5472.CAN-12-0938>
- Lanaya H, Natarajan A, Komposch K, Li L, Amberg N, Chen L, Wculek SK, Hammer M, Zenz R, Peck-Radosavljevic M et al. EGFR has a tumour-promoting role in liver macrophages during hepatocellular carcinoma formation. *Nat Cell Biol* 2014; 16:972-81, 1-7; PMID:25173978; <http://dx.doi.org/10.1038/ncb3031>
- Pellicoro A, Ramachandran P, Iredale JP, Fallowfield JA. Liver fibrosis and repair: immune regulation of wound healing in a solid organ. *Nat*

- Rev Immunol 2014; 14:181-94; PMID:24566915; <http://dx.doi.org/10.1038/nri3623>
33. Ramachandran P, Pellicoro A, Vernon MA, Boulter L, Aucott RL, Ali A, Hartland SN, Snowdon VK, Cappon A, Gordon-Walker TT et al. Differential Ly-6C expression identifies the recruited macrophage phenotype, which orchestrates the regression of murine liver fibrosis. *Proc Natl Acad Sci U S A* 2012; 109:E3186-3195; PMID:23100531; <http://dx.doi.org/10.1073/pnas.1119964109>
  34. Ilkovitch D, Lopez DM. The liver is a site for tumor-induced myeloid-derived suppressor cell accumulation and immunosuppression. *Cancer Res* 2009; 69:5514-21; PMID:19549903; <http://dx.doi.org/10.1158/0008-5472.CAN-08-4625>
  35. Dolcetti L, Peranzoni E, Ugel S, Marigo I, Fernandez Gomez A, Mesa C, Geilich M, Winkels G, Traggiai E, Casati A et al. Hierarchy of immunosuppressive strength among myeloid-derived suppressor cell subsets is determined by GM-CSF. *Eur J Immunol* 2010; 40:22-35; PMID:19941314; <http://dx.doi.org/10.1002/eji.200939903>
  36. Sinha P, Ostrand-Rosenberg S. Myeloid-derived suppressor cell function is reduced by Withaferin A, a potent and abundant component of *Withania somnifera* root extract. *Cancer Immunol Immunother* 2013; 62:1663-73; PMID:23982485; <http://dx.doi.org/10.1007/s00262-013-1470-2>
  37. Corzo CA, Condamine T, Lu L, Cotter MJ, Youn J-I, Cheng P, Cho H-I, Celis E, Quiceno DG, Padhya T et al. HIF-1 $\alpha$  regulates function and differentiation of myeloid-derived suppressor cells in the tumor microenvironment. *J Exp Med* 2010; 207:2439-53; PMID:20876310; <http://dx.doi.org/10.1084/jem.20100587>
  38. Monu NR, Frey AB. Myeloid-Derived Suppressor Cells and anti-tumor T cells: a complex relationship. *Immunol Invest* 2012; 41:595-613; PMID:23017137; <http://dx.doi.org/10.3109/08820139.2012.673191>
  39. Okazaki T, Chikuma S, Iwai Y, Fagarasan S, Honjo T. A rheostat for immune responses: the unique properties of PD-1 and their advantages for clinical application. *Nat Immunol* 2013; 14:1212-8; PMID:24240160; <http://dx.doi.org/10.1038/ni.2762>
  40. Freeman GJ, Long AJ, Iwai Y, Bourque K, Chernova T, Nishimura H, Fitz LJ, Malenkovich N, Okazaki T, Byrne MC et al. Engagement of the Pd-1 immunoinhibitory receptor by a novel B7 family member leads to negative regulation of lymphocyte activation. *J Exp Med* 2000; 192:1027-34; PMID:11015443; <http://dx.doi.org/10.1084/jem.192.7.1027>
  41. Ma C, Kapanadze T, Gamrekelashvili J, Manns MP, Korangy F, Gretten TF. Anti-Gr-1 antibody depletion fails to eliminate hepatic myeloid-derived suppressor cells in tumor-bearing mice. *J Leukoc Biol* 2012; 92:1199-206; PMID:23077247; <http://dx.doi.org/10.1189/jlb.0212059>
  42. Draghiciu O, Lubbers J, Nijman HW, Daemen T. Myeloid derived suppressor cells—An overview of combat strategies to increase immunotherapy efficacy. *OncoImmunology* 2015; 4:e954829; PMID:25949858; <http://dx.doi.org/10.4161/21624011.2014.954829>
  43. Vincent J, Mignot G, Chalmin F, Ladoire S, Bruchard M, Chevriaux A, Martin F, Apetoh L, Rébé C, Ghiringhelli F. 5-fluorouracil selectively kills tumor-associated myeloid-derived suppressor cells resulting in enhanced T cell-dependent antitumor immunity. *Cancer Res* 2010; 70:3052-61; PMID:20388795; <http://dx.doi.org/10.1158/0008-5472.CAN-09-3690>
  44. Qin H, Lerman B, Sakamaki I, Wei G, Cha SC, Rao SS, Qian J, Hailemichael Y, Nurieva R, Dwyer KC et al. Generation of a new therapeutic peptide that depletes myeloid-derived suppressor cells in tumor-bearing mice. *Nat Med* 2014; 20:676-81; PMID:24859530; <http://dx.doi.org/10.1038/nm.3560>
  45. Qin H, Wei G, Gwak D, Dong Z, Xiong A, Kwak LW. Targeting tumor-associated myeloid cells for cancer immunotherapy. *Oncoimmunology* 2015; 4:e983961; PMID:25949898; <http://dx.doi.org/10.4161/2162402X.2014.983761>
  46. Chang C-M, Lo C-H, Shih Y-M, Chen Y, Wu P-Y, Tsuneyama K, Rofler SR, Tao M-H. Treatment of hepatocellular carcinoma with adeno-associated virus encoding interleukin-15 superagonist. *Hum Gene Ther* 2010; 21:611-21; PMID:20064014; <http://dx.doi.org/10.1089/hum.2009.187>